Ferroelectrics, 1992, Vol. 129, pp. 19–30
Reprints available directly from the publisher
Photocopying permitted by license only

ELECTRICALLY INDUCED MECHANICAL VIBRATIONS OF A SURFACE STABILIZED FERROELECTRIC LIQUID CRYSTAL CELL†

N. ÉBER,‡ L. KOMITOV, S. T. LAGERWALL, M. MATUSZCZYK, K. SKARP and B. STEBLER

Physics Department, Chalmers University of Technology, S-41296 Göteborg, Sweden

(Received November 16, 1991)

Electric field induced mechanical vibrations are investigated in an SSFLC cell using a piezoelectric accelerometer. It is shown that vibrations exist both normal and parallel to the confining substrates. Typical waveforms and frequency spectra of the acceleration signal are presented. Dependences of the vibration amplitude on the frequency and amplitude of the applied voltage as well as on the temperature are analysed.

Keywords: Ferroelectrics, liquid crystals, chiral smectics, electromechanical effect, vibrations

INTRODUCTION

Chiral smectic C (S_C^*) liquid crystals have attracted considerable attention in recent years because of their ferroelectric properties. In thin helix-free layers of these compounds a fast, bistable electrooptical switching can be realized.[1] The so called surface stabilized ferroelectric liquid crystal (SSFLC) cells have promising perspectives in the application field as fast light shutters or high information content displays.[2]

It is well known, that alternating electric fields can induce mechanical vibrations in various materials. The most common effect is electrostriction, this being a quadratic phenomenon. Linear effects are less common but may be observed in materials lacking a centre of symmetry (e.g. piezoelectricity in certain crystals, ceramics and polymers).

A linear electromechanical effect in liquid crystals was observed and studied for the first time in the S_C^* phase on sandwich cells when the glass plates coated with the electrodes were not rigidly fixed together nor sealed[3]—this being in contrast to usual liquid crystal display cells. When the plates are not fixed together, the electric field induces a shear flow in the S_C^* substance which results in a lateral vibration of the substrates (i.e., vibration within the plane of the electrodes).[4] This phenomenon has subsequently been studied using S_C^* compounds with various

†Paper presented at the 3rd International Conference on Ferroelectric Liquid Crystals, Boulder, 24–28 June 1991.

‡Permanent address: Central Research Institute for Physics, H-1525 Budapest, P.O. Box 49, Hungary.

physical properties in thick[5–8] as well as in thin cells,[9] moreover it has been detected in polymeric S_C^* liquid crystals.[10,11]

Because liquid crystal display cells are hermetically sealed, one would not expect lateral vibrations. However, such SSFLC cells often generate an audible sound when they are subjected to an AC electric field thereby indicating the presence of mechanical vibrations. Our aim was to study these vibrations by determining their direction and other characteristics. Here we present the first experimental data concerning this phenomenon.

EXPERIMENTAL SET-UP

For experimentally studying mechanical vibrations an ordinary but "loud" SSFLC sandwich cell was chosen. The non-patterned electrodes (45 × 20 mm^2 area) were separated by evaporated SiO spacers to provide 2 μm thickness. Planar orientation was established by oblique evaporation of SiO at 60° incidence to the substrate normal which yields essentially zero pretilt. After assembly, the cell was filled with commercial FLC mixture ZLI-3774 (Merck) in vacuum and it was then sealed hermetically.

The block scheme of our experimental set-up is shown in Figure 1. The cell was mounted in a hot stage and the temperature controlled to within 0.1°C accuracy

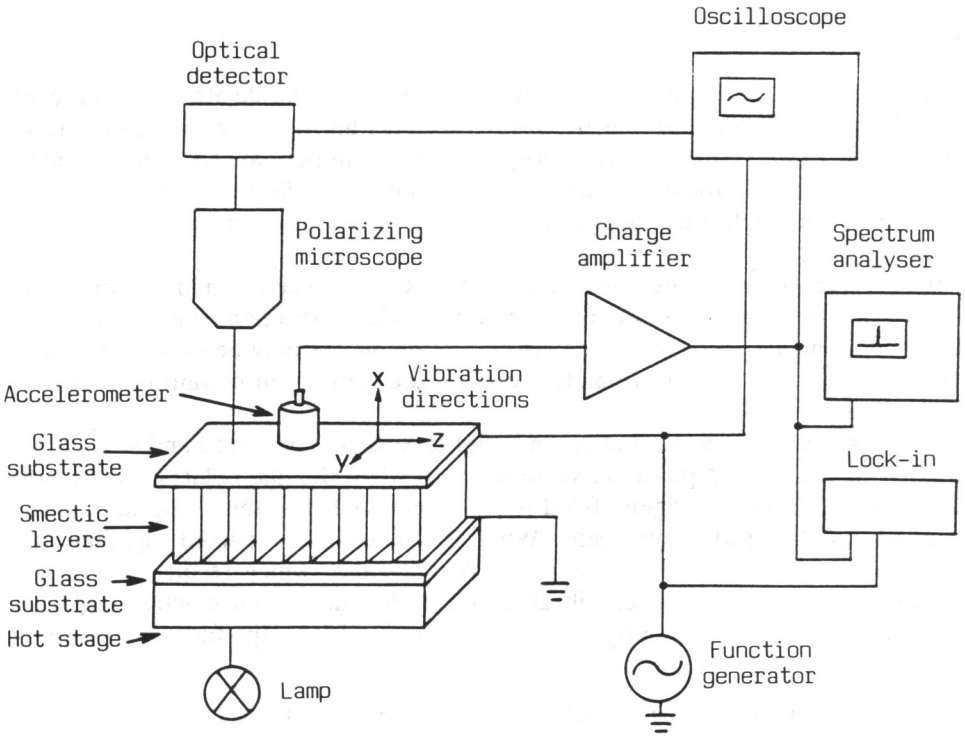

FIGURE 1 Experimental set-up for investigating electrically induced mechanical vibrations of SSFLC cells.

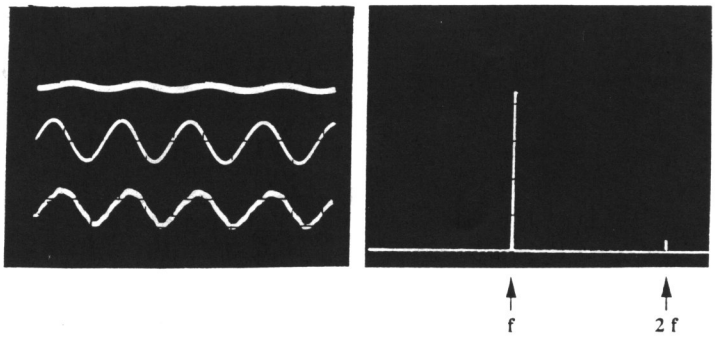

FIGURE 2 Waveforms and frequency spectrum of acceleration for transversal vibrations (along x-axis) of f = 20.42 kHz at applied voltage of U = 2.51 V_{rms} and at T = 22°C. Left: Electrooptical response (top, 0.1 V/div), applied voltage (middle, 5 V/div), acceleration (bottom, 0.2 ms^{-2}/div), sweep 20 μs/div. Right: Amplitude of harmonic components of acceleration (0.02 ms^{-2}/div), sweep 5 kHz/div.

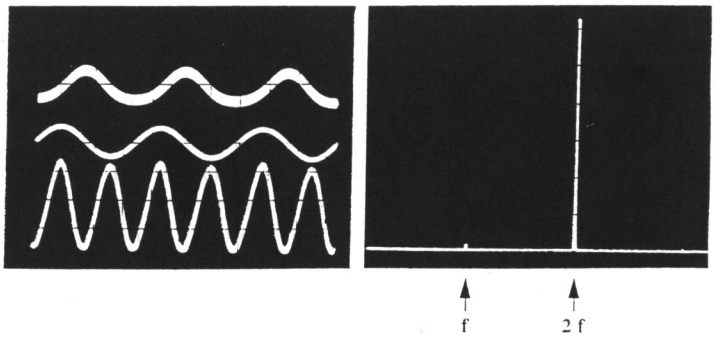

FIGURE 3 Waveforms and frequency spectrum of acceleration for transversal vibrations (along x-axis) of f = 5.76 kHz at applied voltage of U = 3.78 V_{rms} and at T = 22°C. Left: Electrooptical response (top, 0.1 V/div), applied voltage (middle, 10 V/div), acceleration (bottom, 1 ms^{-2}/div), sweep 50 μs/div. Right: Amplitude of harmonic components of acceleration (0.2 ms^{-2}/div), sweep 2 kHz/div.

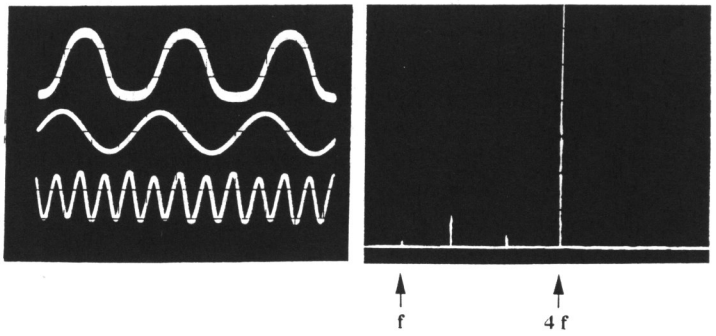

FIGURE 4 Waveforms and frequency spectrum of acceleration for transversal vibrations (along x-axis) of f = 2.88 kHz at applied voltage of U = 5.14 V_{rms} and at T = 22°C. Left: Electrooptical response (top, 0.1 V/div), applied voltage (middle, 10 V/div), acceleration (bottom, 1.6 ms^{-2}/div), sweep 0.1 ms/div. Right: Amplitude of harmonic components of acceleration (0.16 ms^{-2}/div), sweep 2 kHz/div.

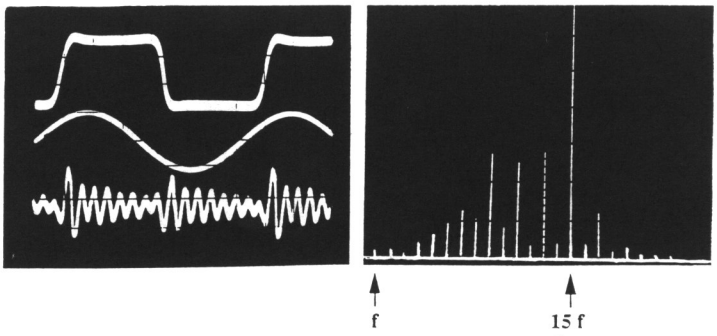

FIGURE 5 Waveforms and frequency spectrum of acceleration for transversal vibrations (along x-axis) of $f = 712$ Hz at applied voltage of $U = 6.96$ V_{rms} and at $T = 22°C$. Left: Electrooptical response (top, 0.1 V/div), applied voltage (middle, 10 V/div), acceleration (bottom, 0.1 ms^{-2}/div), sweep 0.2 ms/div. Right: Amplitude of harmonic components of acceleration (0.01 ms^{-2}/div), sweep 2 kHz/div.

using a Linkam CO600 temperature controller. The sine wave voltage applied to the cell was produced by an ordinary function generator. A piezoelectric accelerometer (Brüel & Kjœr 4344) was fixed by a cyano-acrylate adhesive to the top plate of the cell to serve as a vibration transducer and its output was connected to a charge amplifier (Brüel & Kjœr 2635), this arrangement yielded an electric signal proportional to the acceleration of the top plate of the cell. We were able to achieve a conversion factor of 1000 mV/ms^{-2} in the most sensitive range. The signal was continuously monitored by an oscilloscope and its frequency spectrum was obtained using a Tektronix 5111 storage oscilloscope equipped with a 5L4N spectrum analyser plug-in. The basic and second harmonic components of the acceleration were measured by an EG&G Brookdeal 5206 lock-in amplifier. During the vibration measurements either the texture of the cell could be monitored under a Leitz Ortholux polarizing microscope, or the electrooptical response (transmitted intensity between crossed polars) could be obtained using photodetectors built onto the microscope.

The piezoelectric accelerometer is a strongly anisotropic transducer: in practice it is sensitive only to vibrations along its mounting axis (its transverse sensitivity does not exceed 3%). Thus acceleration measurements were carried out with the mounting axis of the transducer being consecutively fixed in three different orthogonal directions: perpendicular to the substrates (x-axis); parallel to the substrates, parallel to the smectic layers (y-axis) and parallel to the substrates, normal to the smectic layers (z-axis). This allowed complete mapping of the possible vibrational directions (both transversal and lateral) of the SSFLC cell. We have disregarded any internal chevron structure of the sample since it will be of no direct relevance in our discussion.

EXPERIMENTAL RESULTS

On applying an AC voltage (sine wave) to the electrodes of the SSFLC cell we detected an acceleration signal in each position of the mounting axis of the ac-

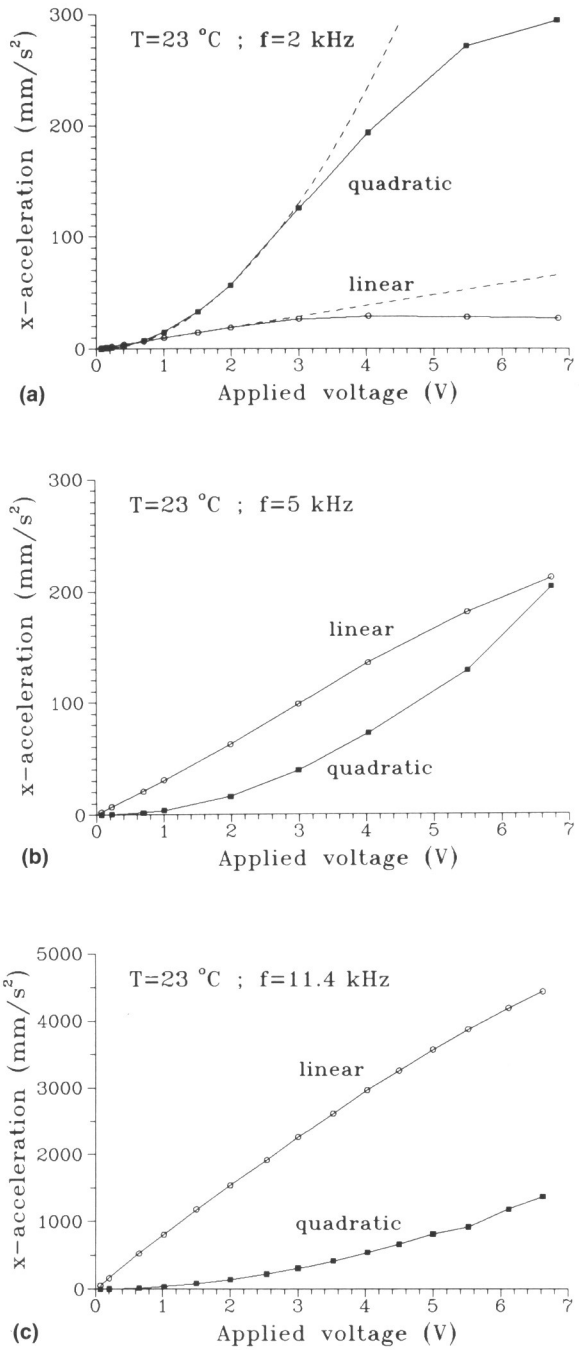

FIGURE 6 Linear and quadratic components of acceleration versus applied voltage for transversal vibrations (along x-axis) at T = 23°C. Dashed lines correspond to the expected behaviour. a) f = 2 kHz; (b) f = 5 kHz; (c) f = 11.4 kHz.

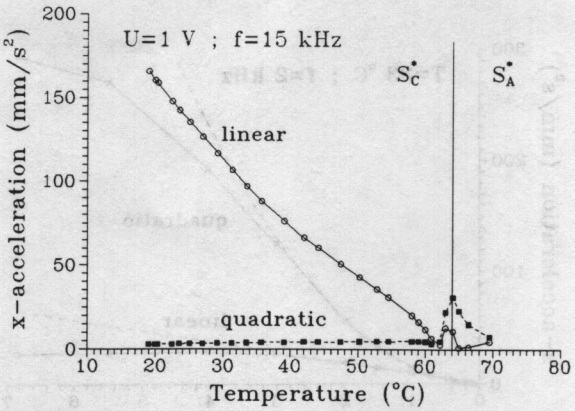

FIGURE 7 Linear and quadratic components of acceleration versus temperature for transversal vibrations (along x-axis) at applied voltage of $U = 1\ V_{rms}$, $f = 15$ kHz.

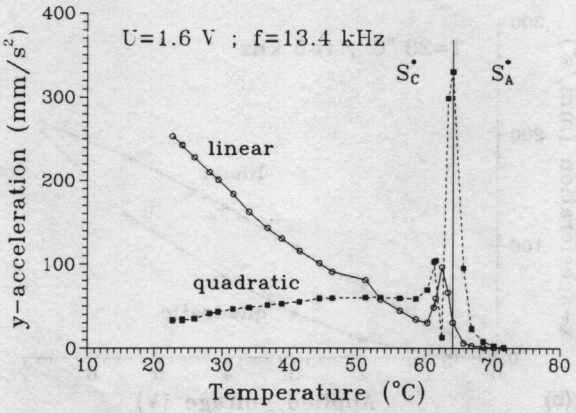

FIGURE 8 Linear and quadratic components of acceleration versus temperature for lateral vibrations along y-axis (along smectic layers) at applied voltage of $U = 1.6\ V_{rms}$, $f = 13.4$ kHz.

celerometer. This proves that the electric field induces mechanical vibrations in all three orthogonal directions.

The electromechanical response of the sample depends strongly on the frequency and amplitude of the applied voltage. For illustration, we present in Figures 2–5 some photos taken from the screen of the oscilloscope and the spectrum analyser at room temperature for transversal (along the x-axis) vibrations. The waveforms in the photos correspond to the electrooptical response (top), the applied voltage (middle), and the acceleration (bottom). The height of the peaks in the frequency spectra corresponds to the amplitude of the various harmonic components of the acceleration.

It can be seen from Figure 2 that at high frequencies and small amplitudes the electromechanical response is almost purely linear while at lower frequencies it may become almost purely quadratic (Figure 3). In both cases the almost purely linear electrooptical response indicates that there is no complete director reorientation. On further decreasing the frequency and increasing the amplitude of the applied voltage the higher frequency components become dominant in the accel-

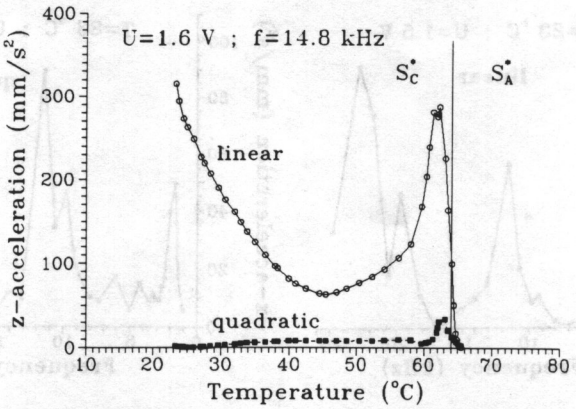

FIGURE 9 Linear and quadratic components of acceleration versus temperature for lateral vibrations along z-axis (normal to smectic layers) at applied voltage of $U = 1.6\ V_{rms}$, $f = 14.8$ kHz.

eration (Figure 4). This will become more evident when entering the bistable switching regime (Figure 5) where the acceleration and the electrooptical signals do not show any similarity. The electromechanical responses shown in Figures 2–5 are, however, not necessarily typical. Over the full frequency range the acceleration signal is generally composed of linear, quadratic and higher harmonic components and the non-linear distortions of the acceleration waveforms increase with increasing applied voltage. We should like to emphasize that the above statements hold for lateral (along the y- and the z-axis) vibrations as well.

In order to obtain more information about the nature of the vibrations we restricted ourselves to investigating the basic and second harmonic (linear and quadratic) components which can be measured separately by lock-in detection.

The dependence of the acceleration on the applied voltage is presented in Figures 6a–c for transversal vibrations. It can be seen that there is a linear increase in the basic harmonic and a quadratic increase in the second harmonic component of the acceleration at small applied voltages, as expected. However, at higher voltages a deviation from this behaviour is observed; this deviation is less pronounced at higher frequencies. Furthermore the relative amplitudes of the basic and second harmonic components are also changing with the frequency in accordance with the trends shown in Figures 2–5. This is in agreement with the fact that at lower frequencies the electric field induced distortion of the director becomes large at smaller voltages thereby representing an internal non-linearity through the anisotropic physical properties of the substance. Similar behaviour was found for lateral vibrations.

The temperature dependence of the acceleration was also measured at voltages below the switching threshold. Figure 7 corresponds to the transversal (along the x-axis) vibrations while Figures 8 and 9 are for the lateral ones along the y-axis and the z-axis, respectively. The temperature dependences of the vibrations in all directions are very similar, the linear accelerations decreasing with increasing temperature in the S_C^* phase except within a narrow range below the S_C^*–S_A^* phase transition. The quadratic components of the acceleration possess a maximum in the same temperature range. The observed peaks are also in general accordance

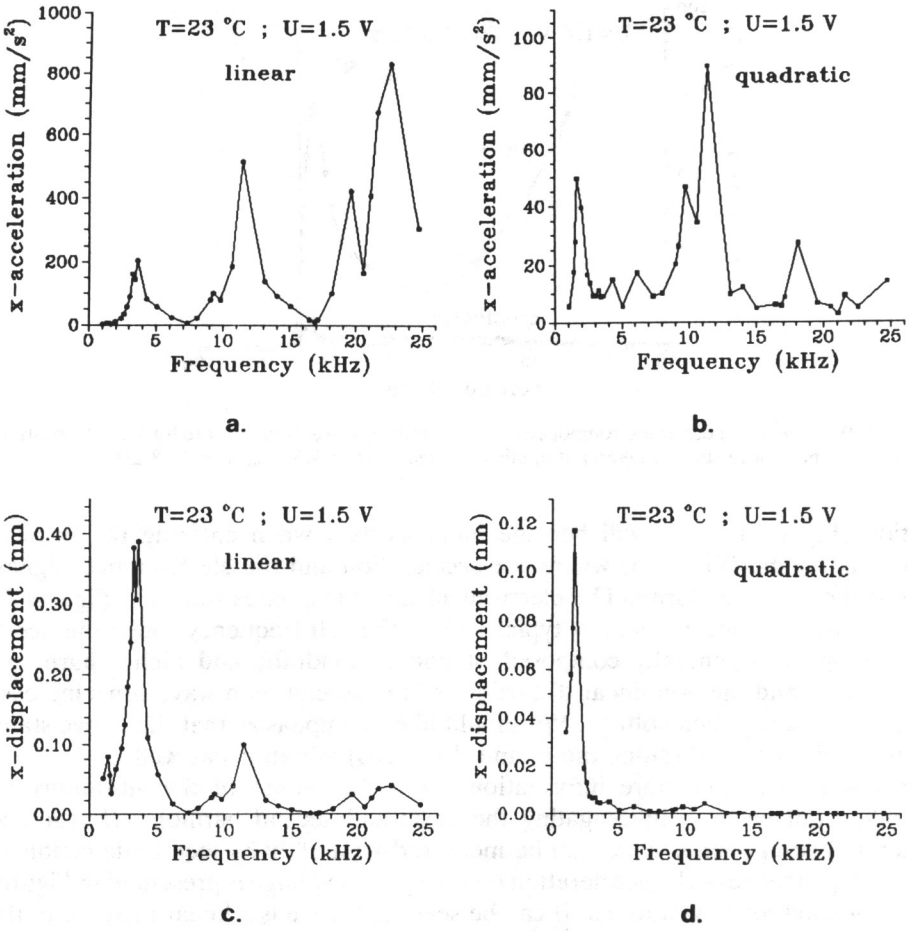

FIGURE 10 Frequency dependence of vibration amplitude for transversal vibrations (along x-axis) at U = 1.5 V and T = 23°C. a) linear component of acceleration; b) quadratic component of acceleration; c) linear component of displacement; and d) quadratic component of displacement.

with a softening of the system at the transition, i.e. with the fact that the mechanical susceptibility increases when the S_C^*–S_A^* transition temperature is being approached from either side. As can be expected from the electroclinic behaviour the vibrations persist in the S_A^* phase just above the transition but cease gradually with further increase in temperature.

Comparison between Figure 8 and 9 shows that for the vibration normal to the layers at the monotonic decrease of the amplitude of the linear response fails even at 20°C below the S_C^*–S_A^* transition. With further increase in temperature the amplitude starts to increase again almost reaching its low temperature value before it falls sharply just before the phase transition. This vibration mainly corresponds to dilation and compression of the layers, i.e. to the soft mode in the case of a simple bookshelf structure without chevrons (as in the sketch in Figure 1). So we can assume that this linear response characterizes the soft mode fairly well; it characterizes it the better, the smaller is the chevron angle, i.e. the more we

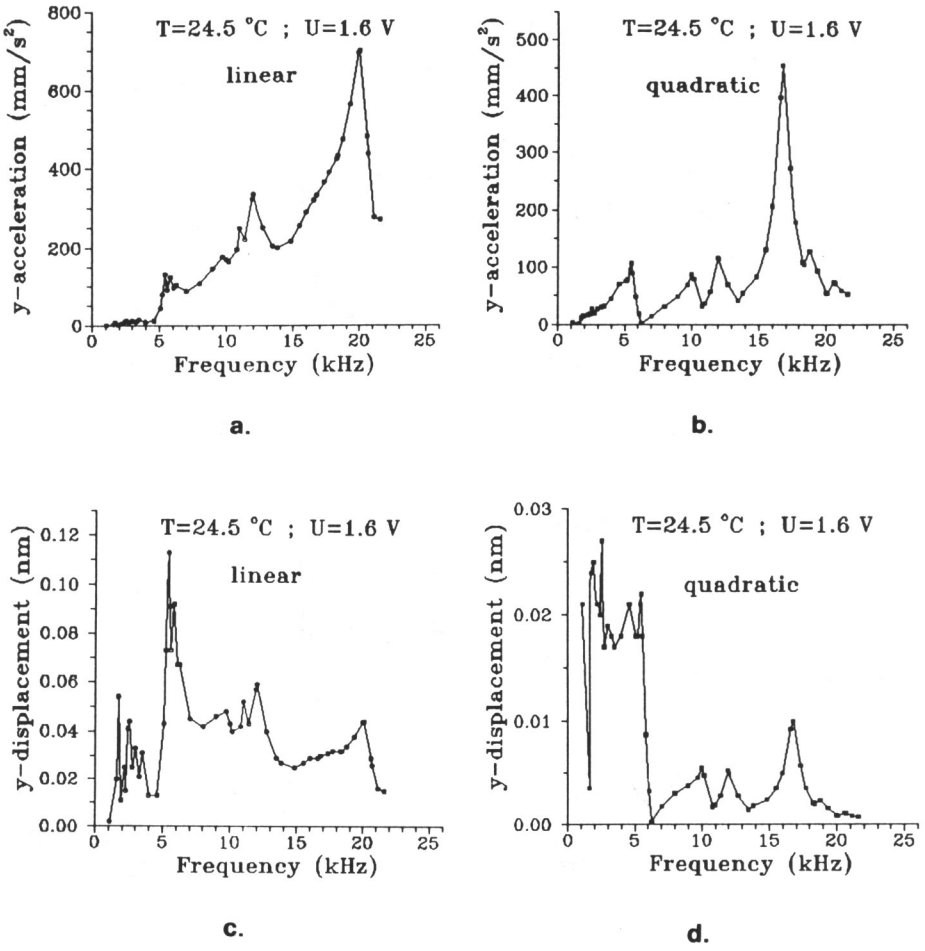

FIGURE 11 Frequency dependence of vibration amplitude for lateral vibrations along *y*-axis (along smectic layers) at U = 1.6 V and T = 24.5°C. a) linear component of acceleration; b) quadratic component of acceleration; c) linear component of displacement; and d) quadratic component of displacement.

approach the transition temperature. The drop in the acceleration just below the transition may thus correspond to the dynamical slowing down of this mode.

It has already been shown (see Figure 2–5) that the vibration characteristics are frequency dependent. In Figures 10–12 we present data on the frequency dependence of the transversal and lateral vibration amplitudes at room temperature and constant amplitude excitation in the 1–25 kHz range. The upper frequency limit of the measurement was chosen much below the internal resonance frequency (>50 kHz) of the transducer in order to have a flat frequency response; the lower frequency limit was determined by the signal to noise ratio.

Several resonance maxima were detected in the 1–25 kHz range. It can be seen from Figures 10–12 that the resonance frequencies for vibrations of different direction did not coincide. We have found that at higher temperatures these resonances tend to shift towards lower frequencies.

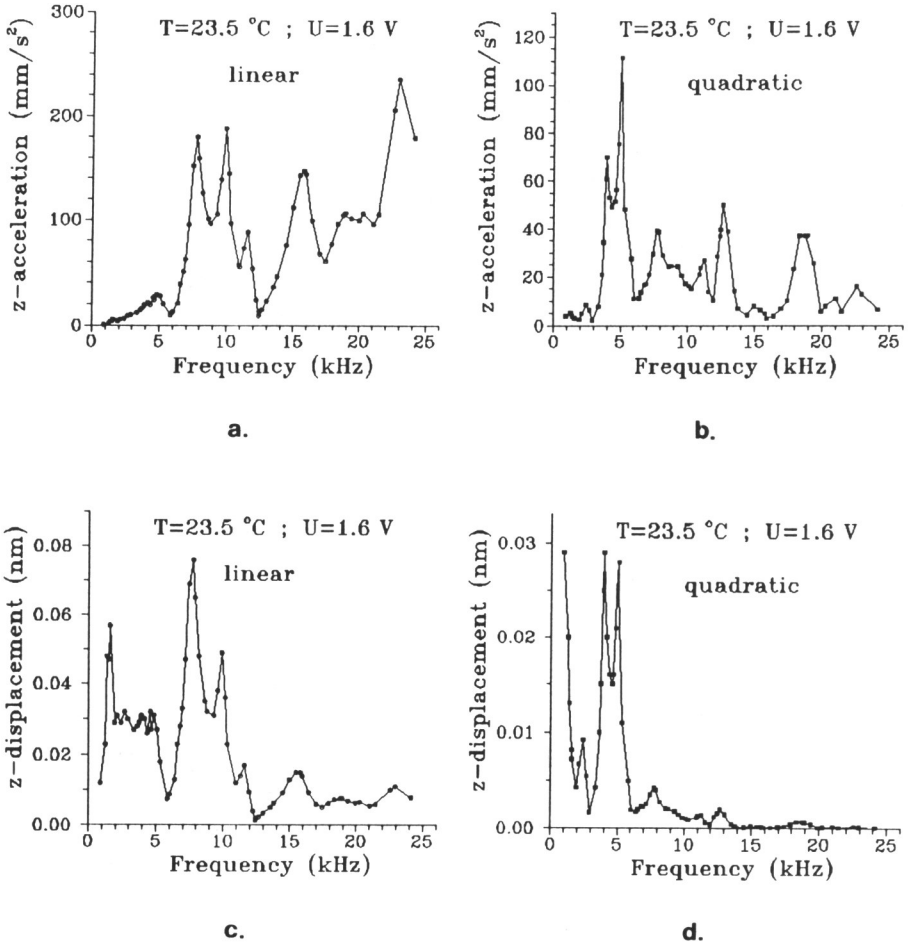

FIGURE 12 Frequency dependence of vibration amplitude for lateral vibrations along z-axis (normal to smectic layers) at U = 1.6 V and T = 23.5°C. a) linear component of acceleration; b) quadratic component of acceleration; c) linear component of displacement; and d) quadratic component of displacement.

Though the directly measured quantity is the acceleration of the top plate of the SSFLC cell, the data can easily be transformed in accordance with the simple relation.

$$\text{displacement} = \text{acceleration}/(2 \cdot \pi \cdot \text{frequency})^2,$$

in order to obtain the displacement amplitudes. In Figures 10–12 the frequency dependence of the displacement amplitudes are shown as well. The rescaling preserves the resonance behaviour of the vibrations, however, it also shows that large high frequency accelerations do not necessarily yield large displacements, whereas almost unmeasurable low frequency accelerations may correspond to fairly large displacements. This points out a drawback in choosing accelerometers to detect vibrations. On the other hand, direct measurement of such low-level, subnanometer displacements does not seem accomplishable.

Finally we would like to emphasize that texture changes including irreversible ones can easily be induced by applying higher voltages or changing the temperature of the SSFLC cell, especially when crossing phase transitions. Despite the vibration amplitudes being very sensitive to these texture changes, they do not change the general characteristics of the phenomenon.

CONCLUSIONS

We have found that AC voltages applied to a hermetically sealed SSFLC cell result in measurable mechanical vibrations in three orthogonal directions. The maximum detected accelerations are of the order of 10 ms^{-2}, the maximum displacements were found to be of the order of 1 nm. Since the sample thickness was 2 μm these amplitudes correspond to only a slight deformation of the sealing material; thus they are not in conflict with the condition of hermetic sealing.

Our observations have shown that there exists a basic harmonic component in the electromechanical response of sealed SSFLC cell due to AC excitation. However, the vibrations cannot be described as purely linear or quadratic effects, rather they should be thought of as a combination of several mechanisms acting together where higher order non-linearities may count as well, especially at higher voltages and lower frequencies. The purely harmonic acceleration signals (see Figures 2–4) could be obtained only if a matching occurred with a certain resonance frequency.

The temperature dependence of the electric field induced mechanical vibrations clearly shows that the linear phenomenon is a peculiarity of the S_C^* phase. The small effect observed in the S_A^* phase just above the S_C^*–S_A^* phase transition may well be due to the electroclinic effect.

The vibrations exhibit definite resonance features. However, these resonances have no influence on the electrooptical response of the cell. The resonance frequencies might correspond to the eigenfrequencies of the mechanical system composed of the glass plates, sealing material, liquid crystal and accelerometer. The presence of zig-zag defects may, however, lead to resonances too.[12] Present data are still not sufficient to enable us to distinguish between the possible causes of resonances.

Our method of detection gives us full information in so far as which vibrations are present. For a more complete analysis of the causes of the vibrations, however, one important element of information is lacking, namely the correlation between the different modes. In order to investigate this correlation we would have to simultaneously measure the three orthogonal vibrations, this would require the use of three separate accelerometers. However, the size of our test display would not allow them to be placed at appropriate positions. Neither could smaller transducers be used because of the corresponding significant loss in sensitivity. Thus it seems preferable that further investigations of the vibrations should be performed on real-size ferroelectric displays.

ACKNOWLEDGEMENT

We wish to thank the Department of Technical Acoustics at Chalmers University of Technology for supplying the accelerometer. This work was supported by the National Swedish Board for Technical

Development, the Swedish Natural Science Research Council and the Swedish Work Environment Fund.

REFERENCES

1. N. A. Clark and S. T. Lagerwall, *Appl. Phys. Lett.*, **36,** 899 (1980).
2. S. T. Lagerwall, N. A. Clark, J. Dijon and J. F. Clerc, *Ferroelectrics,* **94,** 3 (1989).
3. A Jákli, L. Bata, Á. Buka, N. Éber and I. Jánossy, *J. Physique Lett.,* **46,** L-759 (1985).
4. A. Jákli, L. Bata, Á. Buka and N. Éber, *Ferroelectrics,* **69,** 153 (1986).
5. A. Jákli, L. Bata and N. Éber, *Liquid Crystals,* **5,** 1121 (1989).
6. G. Pór and Á. Buka, *J. Physique,* **50,** 783 (1989).
7. A. Jákli and L. Bata, *Ferroelectrics,* **103,** 35 (1990).
8. A. Jákli and L. Bata, *Liquid Crystals,* **7,** 105 (1990).
9. A. Jákli and A. Saupe, Presented at 3rd Int. Conf. Ferroelectric Liq. Cryst., 0–10, Boulder, 1991.
10. A. Jákli and A. Saupe, *Liquid Crystals,* **9,** 519 (1991).
11. N. Éber, L. Bata, G. Scherowsky and A. Schliwa, Presented at 3rd Int. Conf. Ferroelectric Liq. Cryst., 0–44, Boulder, 1991. Preprint KFKI-1991-07/E.
12. A. Jákli, L. Bata and N. Éber, *Ferroelectrics,* **113,** 305 (1991).